Journal of Alloys and Compounds 509 (2011) 8387–8391

Contents lists available at ScienceDirect

Journal of Alloys and Compounds

journal homepage: www.elsevier.com/locate/jallcom

Self-propagating high-temperature synthesis of La(Sr)Ga(Mg,Fe)$O_{3-\delta}$ with planetary ball-mill treatment for solid oxide fuel cell electrolytes

Akira Nobuta[a], Feng-Fan Hsieh[a], Tae Ho Shin[b], Sou Hosokai[a], Satoshi Yamamoto[a], Noriyuki Okinaka[a], Tatsumi Ishihara[b], Tomohiro Akiyama[a,*]

[a] *Center for Advanced Research of Energy and Materials, Faculty of Engineering, Hokkaido University, Sapporo 060-8628, Japan*
[b] *Department of Applied Chemistry, Faculty of Engineering, Kyusyu University, Fukuoka 812-8581, Japan*

ARTICLE INFO

Article history:
Received 29 April 2011
Received in revised form 19 May 2011
Accepted 19 May 2011
Available online 12 June 2011

Keywords:
SHS
SOFC
La(Sr)Ga(Mg,Fe)$O_{3-\delta}$
Planetary ball-mill
Electrolyte

ABSTRACT

This study investigated the combined effects of self-propagating high-temperature synthesis (SHS), planetary ball-mill (PBM) treatment, and sintering temperature on $La_{0.7}Sr_{0.3}Ga_{0.7}Mg_{0.1}Fe_{0.2}O_{3-\delta}$ (LSGMF73712) as an electrolyte material for solid oxide fuel cells (SOFC). The SHS products (SHS-LSGMF73712) were compared with that prepared via solid-state reaction (SSR) in terms of sinterability and power generation performance. The SHS products were treated with PBM for 10, 30, 50, and 70 h. The SHS products contained the by-product $LaSrGaO_4$; however, in the SHS products treated with PBM for longer than 50 h, the by-product disappeared after sintering at 1350 °C for 3 h in air. Among the samples, SHS products treated with PBM for 70 h displayed superior sintering (1350 °C), whereas the SSR product (SSR-LSGMF73712) was successfully sintered at 1450 °C for 3 h in air. Under the cell configuration of Ni–Fe/SHS-LSGMF73712-PBM70 h (0.3 mm thick)/$Sm_{0.5}Sr_{0.5}CoO_3$, the maximum power density was 0.673 W/cm^2 at 800 °C using humidified hydrogen gas (3 mol% H_2O) as a fuel and air as an oxidizing agent at a flow rate of 100 mL/min, which was almost equivalent to that using SSR-LSGMF73712 (0.629 W/cm^2 at 800 °C) under the same conditions.

1. Introduction

Solid oxide fuel cells (SOFC) have attracted worldwide attention as clean power generators with high efficiency, fuel adaptability, and low pollution [1,2]. In particular, perovskite-type oxides are regarded as attractive candidates for electrolyte materials due to their excellent properties, such as high oxide-ion conductivity [3]. Several studies reported that the perovskite-type oxide La(Sr)Ga(Mg)O_3 (LSGM), doped with Sr for the La site and Mg for Ga, has high oxide-ion conductivity [4–6], showing relatively stable electrical conductivity over a wide range of oxygen partial pressures. Doping with Co or Fe for the Ga site of LSGM improves the oxide-ion conductivity, although hole conduction occurs to some extent under high oxygen partial pressures [7,8]. In particular, the application of Fe-doped LSGM greatly improves the power density of the SOFC at lower temperatures [9–11].

Recently, $La_{0.7}Sr_{0.3}Ga_{0.7}Mg_{0.1}Fe_{0.2}O_{3-\delta}$ (LSGMF73712) has been reported as a new attractive substitute for solid electrolytes [12], produced by highly time- and energy-consuming solid-state reaction (SSR) based on calcination. In contrast, self-propagating high-temperature synthesis (SHS), a famous method discovered by Merzhanov in 1967, has been used as an alternative to resolve problems associated with SSR [13,14]. The advantages of SHS are that it does not require additional input energy during the combustion process, uses simple equipment, and occurs via an exothermal reaction [15–17]. In our previous study, we successfully produced LSGMF73712 using the SHS method. The particle sizes of the SHS products were controlled with planetary ball-mill (PBM) treatment, which is critical for the production of extremely fine powders. The SHS and PBM-treated products were then sintered by the spark plasma sintering (SPS) method, in which the sintering temperature of the SHS products was lowered by PBM treatment due to decreased particle size. Therefore, it should be possible to lower the sintering temperature by PBM treatment in traditional sintering.

The purpose of this study was to produce LSGMF73712 by the combination of SHS, PBM, and a traditional sintering method and to examine the power generation performance. The effect of PBM duration and sintering temperature on product sinterability and purity is discussed. The performance of a single cell using SHS-LSGMF73712 is compared with that using SSR-LSGMF73712. These findings will pave the way for practical applications of SOFC using lanthanum gallate as an electrolyte.

---

* Corresponding author. Tel.: +81 11 706 6842; fax: +81 11 726 0731.
E-mail address: takiyama@eng.hokudai.ac.jp (T. Akiyama).

0925-8388/$ – see front matter © 2011 Elsevier B.V. All rights reserved.
doi:10.1016/j.jallcom.2011.05.075

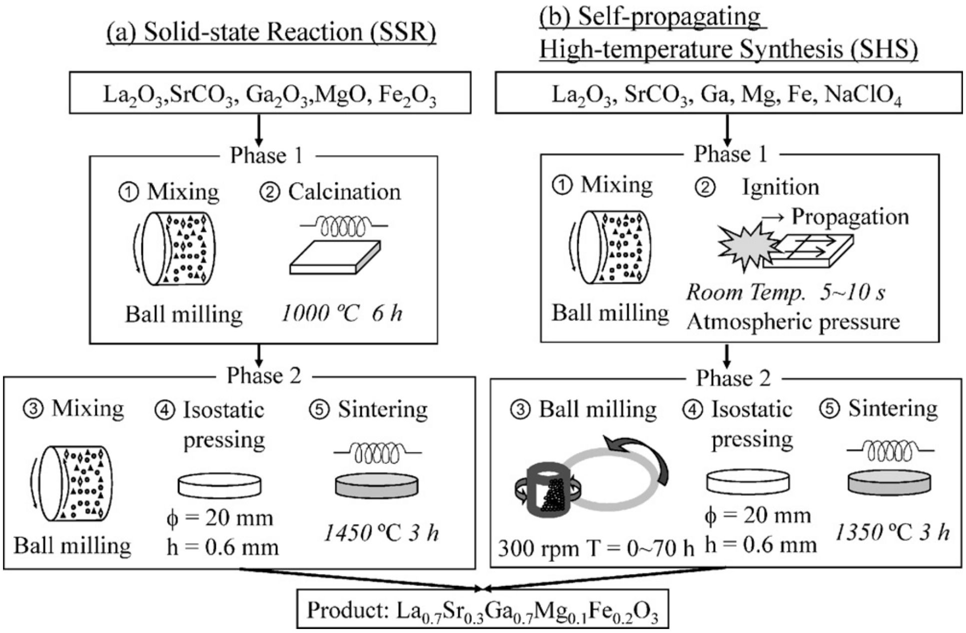

Fig. 1. Comparison of experimental flow between the conventional sintering and SHS for producing La(Sr)Ga(Mg,Fe)O_3. Metallic gallium, magnesium, and sodium perchlorate are used for the exothermic reaction.

2. Experimental

2.1. Sample preparation

Fig. 1 compares the experimental flow between the conventional SSR method and the proposed SHS approach for producing LSGMF73712 samples. In traditional SSR, all the raw materials are oxides or carbonates. In contrast, oxidation of metallic gallium, magnesium, and pure iron by $NaClO_4$ occurred during SHS; commercial powders of La_2O_3 (Aldrich, 99.9% purity), $SrCO_3$ (Aldrich, 99.9% purity), Ga (High Purity Chemical Co. Ltd., 99.9% purity), Mg (High Purity Chemical Co. Ltd., 99.9% purity), Fe (High Purity Chemical Co. Ltd., 99.9% purity), and $NaClO_4$ (Aldrich, 98% purity) were used in this study. First, the raw materials were stoichiometrically mixed in an Al_2O_3-ball mill at 30 rpm for 3 h in air (excessive mixing velocity >30 rpm will cause gallium powder to melt). In typical SSR, the mixed materials are calcined at 1000 °C for 6 h [12]; however, SHS was performed by placing the powder mixture (8 g) in a graphite crucible (20 mm (W) × 30 mm (L) × 7 mm (H)) and supplying Ar gas (99.99 mol%) at atmospheric pressure to the reactor after evacuation by a rotary pump for 10 min. Subsequently, a disposable carbon foil igniter was placed in contact with one end of the powder sample and electrically flashed at 50 V and 100 A at room temperature. The adiabatic temperature (T_{ad}), which was calculated by the adiabatic formula [14], was 2797 °C. When one end of the mixed powders is ignited at the ignition point, the combustion wave propagates to the other end completely with no additional input energy.

The products obtained by SHS were washed using an ultrasonic cleaner to remove the NaCl particles. Next, the SHS products were treated with PBM; the stainless steel mill pot contained stainless steel balls (10 mm in diameter), and PBM treatment was carried out at a rotation speed of 300 rpm with a powder-to-ball mass ratio of 10:1 in air. PBM products were obtained after milling for 10, 30, 50, and 70 h. Finally, all the final samples were identified by X-ray diffraction (XRD) analysis, and the particle size distributions were measured (Horiba, LA-920).

For electrolyte fabrication, the PBM products were isotropically compressed into disks 20 mm in diameter and 0.6 mm thick at 275 MPa in vacuum. The conditions were the same for disks prepared using the SSR method. The calcined SSR samples were sintered at different temperatures ranging from 1350 °C to 1450 °C for 3 h in air to determine the optimal sintering temperature for SSR. In contrast, all the ball-milled SHS products were sintered at 1350 °C for 3 h in air.

2.2. SOFC power generation characteristics

A single-type fuel cell was fabricated using SHS products or SSR products as electrolytes to measure power generation. The disks were polished with diamond wheels to a thickness of 0.3 mm. To measure planer-SOFC power performance using an LSGMF73712 electrolyte, $Sm_{0.5}Sr_{0.5}CoO_{3-\delta}$ (SSC55) was used as a cathode and Ni–Fe as an anode. SSC55 was prepared using the conventional solid state reaction method [18]. For Ni–Fe anode, Ni–Fe (Ni:Fe = 9:1 weight ratio) oxide composite powders were firstly prepared by a conventional wet process method: Fe_3O_4 was loaded on NiO by using $Fe(NO_3)_3$ solution, and then after evaporation of $Fe(NO_3)_3$ solution, the resulting powders were calcined at 673 K for 2 h followed by calcination at 1073 K for 6 h in air. The prepared anode and cathode powders were symmetrically slurry-coated on the each side of LSGMF73712 disk, and then calcined at 1373 K and 1223 K for 1 h in air, respectively. Pt reference electrode was prepared on the side of the cathode by using Pt paste.

The power generation characteristics of a single cell were measured by the four-probe method using humidified hydrogen gas (3 mol% H_2O) as a fuel and air as an oxidizing agent at a flow rate of 100 mL/min, and molten Pyrex glass was used to seal the cells. The current density was controlled with a galvanostat (Hokuto Denko, HA301).

3. Results and discussion

3.1. SHS of LSGMF73712 and ball-mill treatment

The SHS of LSGMF73712 occurred via the exothermic reaction shown below as reaction (1). $NaClO_4$ played an important role as an oxidizing reagent, providing oxygen for the synthesis reaction during SHS. The raw materials were ignited, and the combustion wave propagated to the end of the graphite crucible.

$$\begin{aligned}0.35La_2O_3 &+ 0.3SrCO_3 + 0.7Ga + 0.1Mg + 0.2Fe\\ &+ 0.4125NaClO_4 \rightarrow La_{0.7}Sr_{0.3}Ga_{0.7}Mg_{0.1}Fe_{0.2}O_3\\ &+ 0.3CO_2(g) + 0.4125NaCl(g) \qquad (1)\end{aligned}$$

The sample emitted heat and white smoke due to evaporation of sodium chloride (NaCl) during the SHS process, and then the SHS products were treated with PBM.

Fig. 2 shows the XRD patterns of the SHS products, treated with PBM for different durations, in an argon atmosphere. The main phase was $LaGaO_3$ with no detectable NaCl. However, the second phase, $LaSrGaO_4$, was observed in the XRD patterns of SHS products treated with PBM for short times of less than 30 h; the $LaSrGaO_4$ peaks diminished with increasing PBM time due to the mechanical milling effect. In our previous study, the relationship between the diminished impurity phase ($LaSrGaO_4$) and PBM treatment was examined systematically [19] and revealed that the quantity of $LaSrGaO_4$ gradually disappeared with increasing PBM time. This is explained by the amorphous crystal structure and the

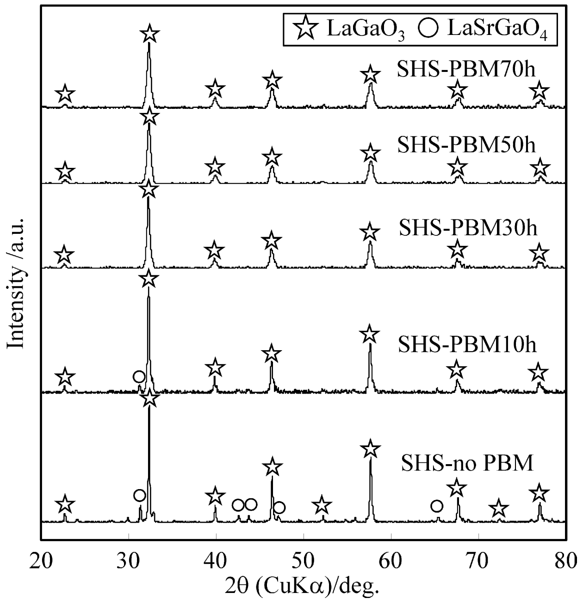

Fig. 2. XRD patterns of the products after SHS in an Ar atmosphere with different planetary ball-milling times. PBM: planetary ball milling; SHS: self-propagating high-temperature synthesis.

peak-broadening effect due to PBM treatment. As discussed above, the SHS products treated with PBM for longer than 50 h were composed of $LaGaO_3$ in which Sr, Mg, and Fe were highly dispersed.

The average particle size of SHS products decreased with increasing PBM time. The mean particle size of the SHS product without PBM treatment was approximately 12.7 μm, and the samples that were ball-milled for 10, 30, 50, and 70 h were approximately 5.3, 4.4, 3.2, and 4.6 μm in diameter, respectively. The average particle size of the SHS product that was ball-milled for 70 h (SHS–PBM70 h) was larger than that of the SHS product that was ball-milled for 50 h (SHS–PBM50 h) due to agglomeration caused by the high surface energy of the fine powders. Accordingly, the primary particle size of the SHS–PBM70 h powder was likely much smaller than that of the other powder samples.

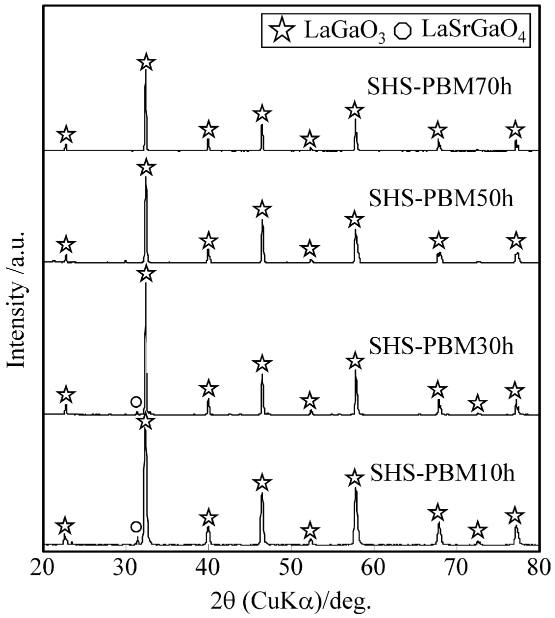

Fig. 3. XRD patterns of the products prepared by SHS, planetary ball milling for different durations, and sintering at 1350 °C for 3 h in air. PBM: planetary ball milling; SHS: self propagating high-temperature synthesis.

3.2. *Sintering of LSGMF73712 after SHS*

Fig. 3 compares the XRD patterns of SHS products treated with PBM for different durations and sintered at 1350 °C for 3 h in air. The patterns mainly consist of peaks from the $LaGaO_3$ perovskite phase. Some weak peaks assigned to $LaSrGaO_4$ were observed in the XRD patterns of $LaGaO_3$-based oxides treated with PBM for less than 30 h. In contrast, SHS samples that were treated with PBM for longer than 50 h and sintered differed from SHS–PBM10 h and SHS–PBM 30 h. No second phase, $LaSrGaO_4$, was detected in their XRD patterns. That is, by-products were not generated during sintering.

Fig. 4 shows photographs of the products treated with PBM for different durations before and after sintering. The color of the SHS

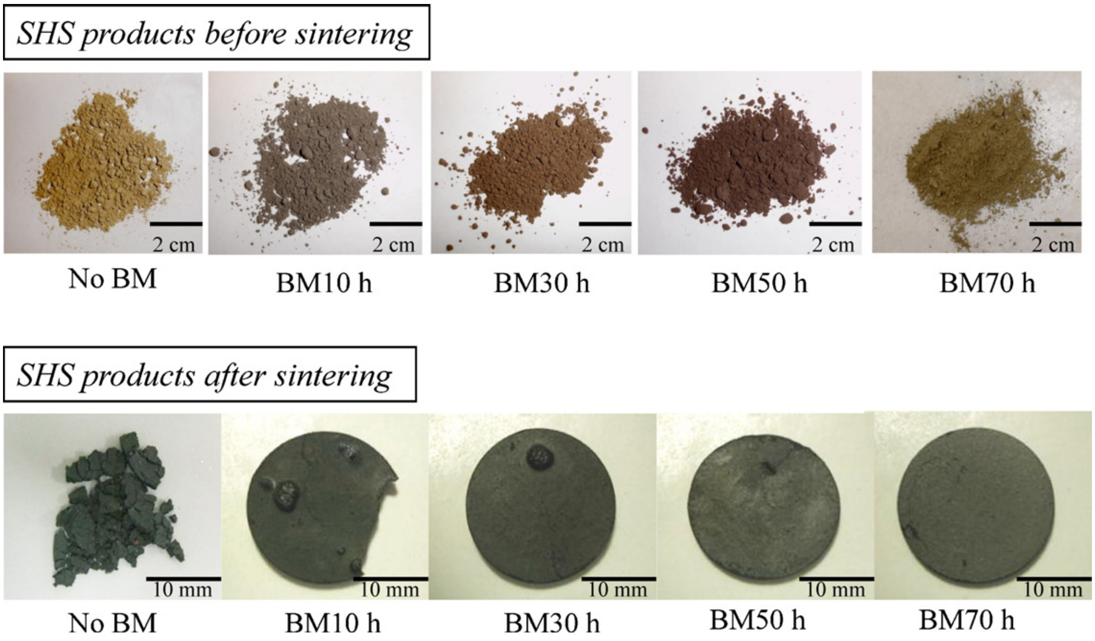

Fig. 4. Photographs of the samples prepared with different planetary ball-milling times before and after sintering. BM: ball milling.

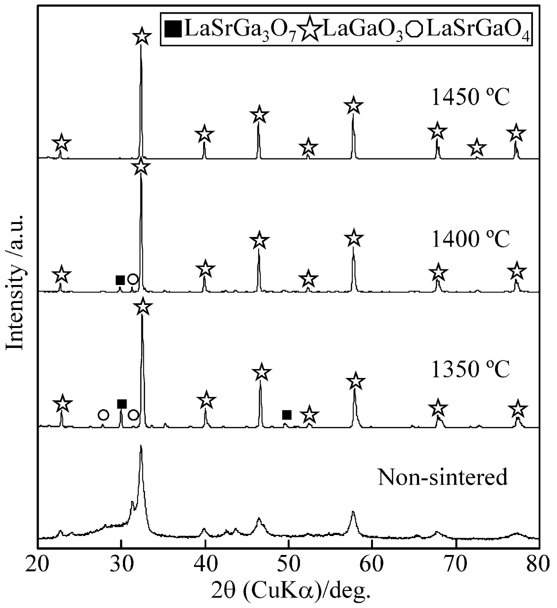

Fig. 5. XRD patterns of LSGMF73712 first prepared by traditional solid-state reaction (SSR) and sintered at different temperatures for 3 h in air.

products changed gradually from light brown to dark brown with increasing PBM time from 0 to 50 h, and then changed to brown again at a PBM time of 70 h before sintering. However, the color of all samples changed to deep gray after sintering.

All SHS samples were heated at 1350 °C for 3 h in air, and, as a result, both SHS–PBM50 h and SHS–PBM70 h were successfully sintered with no cracks, although SHS–PBM samples showed apparent segregation. In contrast, the SHS products that were treated with PBM for 10 h (SHS-PBM10 h) and 30 h (SHS-PBM30 h) had major cracks because of unreacted LaSrGaO$_4$, and the SHS products that were not treated with PBM were not sintered at all. In conclusion, the SHS–PBM70 h sample exhibited superior sinterability among all the fine powders.

3.3. XRD phase analysis of LSGMF73712 fabricated by SSR

Fig. 5 shows the XRD patterns of samples produced by traditional SSR, which were sintered at different temperatures ranging from 1350 °C to 1450 °C for 3 h in air. The samples sintered at lower temperatures (1350–1400 °C) still had secondary phases of LaSrGaO$_4$ and LaSrGa$_3$O$_7$. In contrast, the product sintered at the highest temperature (1450 °C) showed clear phase differences and had strong peaks in the XRD pattern due to a single phase (LaGaO$_3$), indicating that the sample was LSGMF73712.

Table 1 shows the bulk density of SHS products treated with PBM for different durations with that of the SSR products after sintering. The bulk density of sintered samples increased with increasing PBM time. This confirmed that the SHS–PBM50 h and SHS–PBM70 h samples were well sintered at only 1350 °C for 3 h; however, the same sintering conditions were not sufficient for the SSR sample. This can be explained by the fact that the SHS–PBM samples were finer powders of the perovskite phase than the SSR sample; thus, the SHS–PBM samples had a greater propensity for sintering. An advantage of the SHS–PBM method is that the sintering temperature was lowered by 100 °C compared to the SSR method. Therefore, we concluded that short PBM treatment after SHS or lower sintering temperatures in SSR might cause the formation of impurities such as LaSrGaO$_4$ and LaSrGa$_3$O$_7$ in the products. The SHS–PBM samples were successfully sintered by the conventional sintering method at a lower sintering temperature compared to the SSR samples.

3.4. Power generation characteristics of SOFC using LSGMF73712 as an electrolyte

Fig. 6(a) shows the power generation characteristics, *I–V* and *I–P* curves, of the Ni–Fe/SHS–PBM70 h (0.30 mm thick)/SSC55 cell configuration, which was operated at 700 °C and 800 °C. The cell achieved an open circuit voltage (OCV) of 0.840 V at 800 °C. The OCV

Table 1
Bulk density of the SHS products with different PBM periods after sintering process.

Sample	SHS sample PBM10 h	SHS-PBM30 h	SHS-PBM50 h	SHS-PBM70 h	SSRLSGMF[a]
Bulk density (g/cm^3)	5.655	6.058	6.085	6.180	5.609

[a] Sample obtained from solid-state reaction method at 1450 °C.

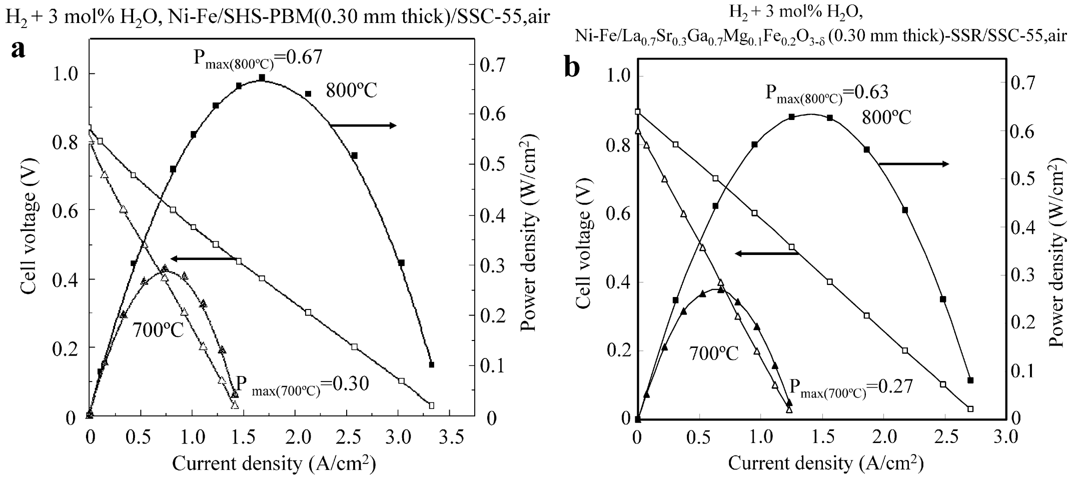

Fig. 6. (a) Power generation curves of the cell using the SHS-PBM 70 h sample as an electrolyte (obtained from self-propagating high-temperature synthesis (SHS)), Ni–Fe as an anode, and Sm$_{0.5}$Sr$_{0.5}$CoO$_{3-\delta}$ (SSC-55) as a cathode. (b) Power generation curves of the cell using the LSGMF73712 sample sintered at 1500 °C as an electrolyte (obtained from solid-state reaction (SSR)), Ni–Fe as an anode, and Sm$_{0.5}$Sr$_{0.5}$CoO$_{3-\delta}$ (SSC-55) as a cathode.

was slightly smaller than the theoretical value, whereas the power density at 800 °C reached a maximum value of $P = 0.673\,\mathrm{W/cm^2}$ at $I = 1.7\,\mathrm{A/cm^2}$. As the operating temperature decreased from 800 °C to 700 °C, the maximum power density became $P = 0.295\,\mathrm{W/cm^2}$ at $I = 0.75\,\mathrm{A/cm^2}$.

Fig. 6(b) shows the power generation characteristics, *I*–*V* and *I*–*P* curves, of the Ni–Fe/LSGMF73712 (0.30 mm thick)/SSC55 cell. The sample used as an SOFC electrolyte was obtained by conventional SSR and sintered at 1450 °C. At 800 °C, the OCV of the cell was 0.894 V, and the power density reached a maximum value of $P = 0.629\,\mathrm{W/cm^2}$ at $I = 1.4\,\mathrm{A/cm^2}$. When the operating temperature decreased from 800 °C to 700 °C, the maximum power density also decreased to $P = 0.270\,\mathrm{W/cm^2}$ at $I = 0.7\,\mathrm{A/cm^2}$.

Comparison between the power density of the cells using SHS–PBM70 h and SSR–LSGMF73712 revealed that the SHS–PBM70 h electrolyte achieved a higher power density despite its lower OCV. This can be explained by the fact that SHS–PBM70 h has a lower electrolyte resistance than that of SSR–LSGMF73712 ($0.24\,\Omega\mathrm{cm^2}$ for SHS–PBM70 h and $0.34\,\Omega\mathrm{cm^2}$ for SSR–LSGMF73712 at 800 °C from *I*–*V* plot in Fig. 6(a) and (b)) because the difference of cell preparation procedures was only fabrication of the electrolyte. However, we cannot put an emphasis that SHS–PBM70 h is better than SSR–LSGMF73712 because the values are not well investigated whether the difference is margin of error. Therefore, SHS–PBM70 h is almost equivalent to SSR–LSGMF73712 in terms of the power density, and highly interesting as an electrolyte for SOFC within a reduced temperature range.

4. Conclusions

To fabricate LSGMF73712, SHS products were pulverized by planetary ball-mill treatment and sintered by a traditional sintering process into the form of disks to evaluate their power generation performance. The results using SHS were compared with those using the traditional SSR method. The results obtained are as follows:

(1) XRD analysis identified the main phase of the product, which was obtained by SHS in an argon atmosphere, as $LaGaO_3$-based material.
(2) When the planetary ball-milling time was longer than 50 h, the sintering temperature was lowered to 1350 °C, which was 100 °C lower than that of the SSR–LSGMF73712.
(3) Under the cell configuration of Ni–Fe/SHS-PBM70 h (0.3 mm thick)/$Sm_{0.5}Sr_{0.5}CoO_{3-\delta}$, OCV was 0.84 V, and maximum power density at 800 °C reached $0.673\,\mathrm{W/cm^2}$. This was almost equivalent to SSR-LSGMF73712 ($P = 0.629\,\mathrm{W/cm^2}$ at 800 °C) under the same conditions.

The combination of SHS and PBM is an attractive method for producing an Fe-doped $LaGaO_3$ electrolyte for intermediate-temperature SOFC. Further studies using other dopants in $LaGaO_3$ electrolytes should be conducted in the future.

Acknowledgement

This study was partially supported by the Ministry of Environment, “Production of PyroCoking-derived Wooden BioCoke and Development of Its SOFC Power Generation” (2006–2008).

References

[1] H.C. Yu, F. Zhao, A.V. Virkar, K.Z. Fung, J. Power Sources 152 (2005) 22–26.
[2] Z. Yang, G. Xia, J.W. Stevenson, J. Power Sources 160 (2006) 1104–1110.
[3] T. Takahashi, H. Iwahara, Energy Convers. 11 (1971) 105.
[4] T. Ishihara, H. Matsuda, Y. Takita, J. Am. Chem. Soc. 116 (1994) 3801.
[5] T. Ishihara, H. Matsuda, Y. Takita, Solid State Ionics 79 (1995) 147.
[6] M. Feng, J.B. Goodenough, Eur. J. Solid State Inorg. Chem. 31 (1994) 663.
[7] T. Ishihara, H. Furutani, M. Honda, T. Yamada, T. Shibayama, T. Akbay, N. Sakai, H. Yokokawa, Y. Takita, Chem. Mater. 11 (1999) 2081.
[8] T. Ishihara, T. Shibayama, M. Honda, H. Nishiguchi, Y. Takita, J. Electrochem. Soc. 147 (2000) 1332–1337.
[9] T. Ishihara, T. Shibayama, H. Nishiguchi, Y. Takita, J. Mater. Sci. 36 (5) (2001) 1051.
[10] T. Ishihara, T. Akbay, H. Furutani, Y. Takita, Solid State Ionics 113–115 (1998) 585.
[11] Z.G. Bi, B.L. Yi, Z.W. Wang, Y.G. Dong, H.J. Wu, Y.C. She, M.J. Cheng, Electrochem. Solid-State Lett. 7 (2004) A105.
[12] T. Ishihara, M. Ando, M. Enoki, Y. Takita, J. Alloys Compd. 408–412 (2006) 507–511.
[13] A.G. Merzhanov, in: C.N.R. Rao (Ed.), Chemistry of Advanced Materials, Blackwell, Oxford, 1992, pp. 19–39.
[14] Z.A. Munir, Am. Ceram. Soc. Bull. 67 (2) (1998) 342–349.
[15] T. Akiyama, Y. Hirai, N. Ishikawa, Mater. Trans. 42 (2001) 460.
[16] H. Ishikawa, M. Enoki, T. Ishihara, T. Akiyama, Mater. Trans. 147 (2006) 149–155.
[17] H. Ishikawa, M. Enoki, T. Ishihara, T. Akiyama, J. Alloys Compd. 430 (2007) 246–251.
[18] T. Ishihara, M. Honda, T. Shibayama, H. Nishiguchi, Y. Takita, J. Electrochem. Soc. 145 (1998) 3177.
[19] F.F. Hsieh, N. Okinaka, T. Akiyama, J. Alloys Compd. 484 (2009) 747–752.